



OPEN Towards novel liver injury therapies based on design, synthesis and therapeutic efficacy of novel sulfone bis-compound on liver necrosis

Huda R. M. Rashdan¹✉, Sarah Hassan², Sara Maher³ & Hend Okasha⁴

Liver necrosis is the irreversible loss of hepatocytes through toxin-induced injury, ischemia, or infection to produce organ dysfunction. It is a significant pathological marker in many liver disorders, including cirrhosis, and hepatitis, and contributes to organ failure and general systemic effects. This research aims to evaluate the protective effects of a newly synthesized compound named 1-(5-((1-(1-(4-((4-(1-((5-acetyl-3-phenyl-1,3,4-thiadiazol-2(3H)-ylidene)hydrazono)ethyl)-5-methyl-1H-1,2,3-triazol-1-yl)phenyl)sulfonyl)phenyl)-5-methyl-1H-1,2,3-triazol-4-yl)ethylidene)hydrazono)-4-phenyl-4,5-dihydro-1,3,4-thiadiazol-2-yl)ethan-1-one (TTTE) sulfone-bis chalcone derivative on liver necrosis caused by TAA therapy using murine model. The research investigates optimal cellular pathways which demonstrate the therapeutic properties of TTTE as a potential treatment for liver injuries. The newly prepared compound TTTE was successfully characterized by Fourier transform infrared spectroscopy (FT-IR), proton nuclear magnetic resonance (1H-NMR) spectroscopy, carbon-13 nuclear magnetic resonance (13C-NMR). The safety of the as-prepared compound TTTE was determined based on weight changes and the behaviors in all the groups were monitored for 21 days. The effect of treatment of TTTE at different doses (300, 200, and 100 mg/kg B.W.) was studied. High-dose TTTE revealed a 62.5% survival rate compared to the untreated TAA group (40%). Molecular analysis exhibited that high-dose TTTE downregulated Cas-3, TIMP-1, and proinflammatory cytokines (TNF- α , NF- κ B, and IL-6) compared to untreated TAA. Results of histopathological and IHC examinations exhibited high TTTE dose have no signs of liver injury with suppression in TGF- β expression as a result of anti-inflammatory response. Our study concluded that the synthesized compound, TTTE has a potential therapeutic strategy in mitigating liver necrosis.

Keywords Sulfone bis-compound, TAA, Liver necrosis, Inflammation, Apoptosis

Liver diseases cause substantial worldwide health problems due to their annual toll of more than 2 million deaths. Cirrhosis-related complications alone cause 1 million deaths each year, while the other 1 million fatalities consist mainly of viral hepatitis and hepatocellular carcinoma¹. The World Health Organization (WHO) recognizes chronic liver conditions such as viral hepatitis, alcoholic liver disease, nonalcoholic fatty liver disease (NAFLD), and cirrhosis as leading causes of global morbidity and mortality^{2,3}. The Middle East experiences high rates of liver diseases because hepatitis B and C virus infections are widespread, while metabolic syndrome and NAFLD incidents continue to rise. Studies throughout the region indicate hepatitis C virus infection is the leading cause of chronic liver disease, cirrhosis, and hepatocellular carcinoma in numerous Middle Eastern nations⁴. These conditions are often associated with hepatic necrosis, a pathological process involving extensive inflammation or direct hepatocellular toxicity that can lead to progressive liver dysfunction and fibrosis (Fig. 1

¹Chemistry of Natural and Microbial Products Department, Pharmaceutical and Drug Industries Research Institute, National Research Centre, 33 El Buhouth St, Dokki, Giza 12622, Egypt. ²Electron Microscopy Department, Theodor Bilharz Research Institute, Giza, Egypt. ³Immunology Department, Theodor Bilharz Research Institute, Giza, Egypt. ⁴Biochemistry and Molecular Biology Department, Theodor Bilharz Research Institute, Giza, Egypt. ✉email: hudadawoud20@yahoo.com

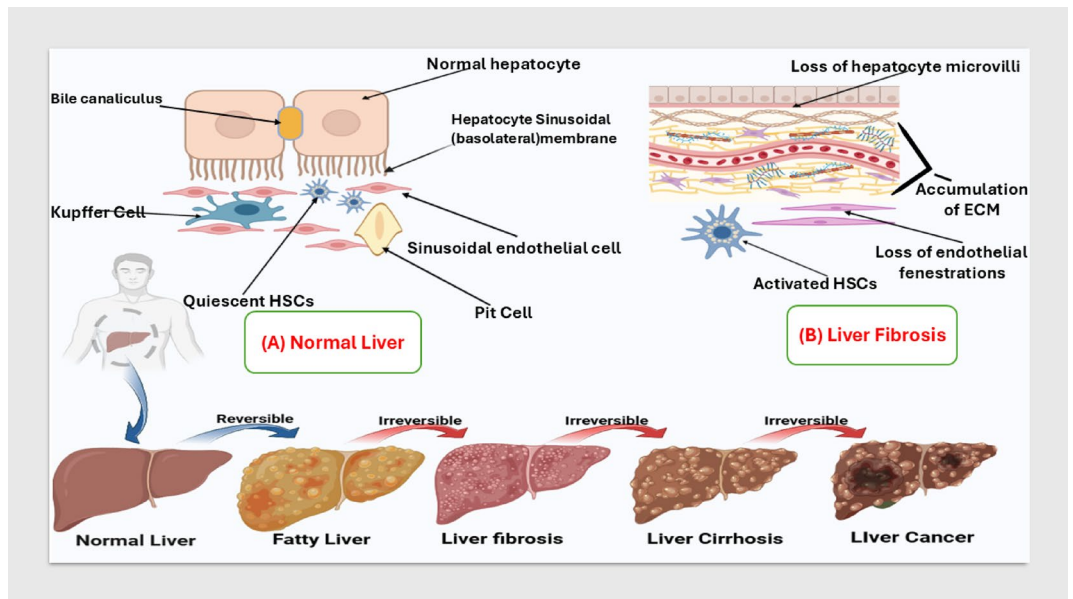


Fig. 1. Normal and fibrotic liver architecture.

Liver fibrosis can be considered a pathogenic case that leads to the loss of the architecture of the liver tissue and excessive accumulation of the extracellular matrix proteins (ECM). The resulting damaged liver tissues limit and alter the vital processes of the liver. This pathogenic case is caused by repeated and various insults to the liver likewise viral infections (chronic hepatitis B or C virus), parasitic or fungal infections, lipid accumulations, iron overload, chronic inflammations, genetical metabolic disorders, prolonged exposure to toxic agents, longterm and intense intake of some drugs (for instance; methyldopa, isoniazid, and chlorpromazine)^{5–7}.

Moreover, liver necrosis may be caused by chronic alcoholism, viral hepatitis B and C, autoimmune diseases, drug toxicity (notably from acetaminophen overdose), and ischemic injury^{8,9}. Managing liver necrosis is difficult and is based on identifying the exact cause of the disease^{10–12}.

Liver necrosis activates the release of damage-associated molecular patterns (DAMPs) together with pro-inflammatory cytokines that include tumor necrosis factor- α (TNF- α), interleukin-1 beta (IL-1 β), IL-6, and transforming growth factor-beta 1 (TGF- β 1). These mediators play essential roles during hepatic stellate cell (HSC) activation. Kupffer cells and other immune cells produce these cytokines after DAMPs are released from necrotic hepatocytes, creating a pro-fibrogenic microenvironment. The potent fibrogenic protein TGF- β 1 makes HSCs change from their quiescent state into an activated myofibroblast-like form, which shows augmented proliferation behavior and advanced migration abilities and generates excessive ECM. Remodeling of ECM and further HSC activation occur through the dual mechanisms of matrix metalloproteinases (MMPs) and reactive oxygen species (ROS) enzymes that develop during necrosis. HSCs become more susceptible to TGF- β 1 after exposure to Toll-like receptor 4 (TLR4) signals, which boost fibrogenic processes. The combined inflammatory signals released during necrosis and cellular stresses lead to HSC activation, which sustains liver fibrosis^{6,13,14}.

The prognosis for patients with liver necrosis remains limited, with mortality rates varying significantly depending on the cause and extent of liver damage¹⁵. Notably, the detection and intervention are crucial in improving outcomes, highlighting the need for continued research into effective therapies and preventive measures for this severe liver condition.

Currently, available treatments for liver necrosis are mainly supportive and focus on managing complications rather than reversing hepatocellular damage or fibrosis progression. Most pharmacological options offer limited efficacy in modulating the underlying apoptotic, inflammatory, and fibrotic pathways. Therefore, there is a critical unmet need for novel compounds that can target multiple aspects of liver injury, including oxidative stress, inflammation, apoptosis, and fibrosis.

Sulfone bis-compounds possess distinctive chemical and biological properties that make them promising candidates for treating liver necrosis. Sulfone serves as a stable moiety that binds to both enzymes as well as signaling proteins associated with oxidative stress and inflammation. Previous studies on polyphenolic tricyclic sulfones act as allosteric inhibitors of liver pyruvate kinase, causing a recorded protection against metabolic stress in liver cells, which concludes that sulfone-containing compounds can modulate liver-specific enzymes and pathways. Furthermore, sulfone bis-compounds may influence signaling pathways related to apoptosis and cellular repair, supporting hepatocyte survival and regeneration^{16,17}.

In light of these properties, **TTTE**—a newly synthesized sulfone bis-chalcone derivative—was designed to address the limitations of current therapies by simultaneously targeting key molecular mechanisms involved in liver injury.

This work was planned to determine the effectiveness of sulfone bis-compound at various concentrations in the treatment of liver necrosis and to determine the capacity of this compound to reduce the extent of

biochemical inflammatory markers, as well as the overall histological alterations in the liver tissue. This approach was designed to provide information on the potential of **TTTE** as a therapeutic agent in treating liver necrosis and its progression to other severe liver diseases.

Materials and methods

Chemistry

Raw materials

Methyl hydrazinecarbodithioate, and Dapsone were procured from Sigma-Aldrich. Some reagents and solvents were used in this study like DMF, Diisopropylethylamine, Absolute ethanol, isopropyl alcohol 99%, and acetic acid 99.9% were imported also from Sigma-Aldrich, Milwaukee, USA. All the solvents and chemicals were used without further purification.

Instrumentation

All melting points were uncorrected and measured using an electrothermal device. The IR spectra were recorded (KBr discs) using a Shimadzu FT-IR 8201 PC spectrophotometer. ^1H - and ^{13}C -NMR spectra were recorded in $(\text{CD}_3)_2\text{SO}$ solutions on a BRUKER 500 FT-NMR system spectrometer, and chemical shifts are expressed in ppm units using TMS as an internal reference.

Synthesis

A mixture of $-2-(1-(5\text{-methyl-}1-(4-((4-(5\text{-methyl-}1-(2-((\text{methylthio})\text{carbonothioyl})\text{hydrazono})\text{ethyl})-1\text{H-}1,2,3\text{-triazol-}1\text{-yl})\text{phenyl})\text{sulfonyl})\text{phenyl})-4,5\text{-dihydro-}1\text{H-}1,2,3\text{-triazol-}4\text{-yl})\text{ethylidene})\text{hydrazine-}1\text{-carbodithioate}$ (**CPSC**) (**1**)^{18,19} (3.36 gm, 5 mmol) and $\text{N}-(\text{phenyl})-2\text{-oxopropanehydrazono-yl chloride}$ (**2**) (2.41 gm, 10 mmol) were heated under reflux in 20 mL ethanol containing catalytic amount of **DIPEA** (2–3 drops) for 5 h. The solid formed was separated and recrystallized from dioxane to give the desired compound.

$1-(5-((1-(1-(4-((4-(1-(5\text{-acetyl-}3\text{-phenyl-}1,3,4\text{-thiadiazol-}2(3\text{H})\text{-ylidene})\text{hydrazono})\text{ethyl})-5\text{-methyl-}1\text{H-}1,2,3\text{-triazol-}1\text{-yl})\text{phenyl})\text{sulfonyl})\text{phenyl})-5\text{-methyl-}1\text{H-}1,2,3\text{-triazol-}4\text{-yl})\text{ethylidene})\text{hydrazono})-4\text{-phenyl-}4,5\text{-dihydro-}1,3,4\text{-thiadiazol-}2\text{-yl})\text{ethan-}1\text{-one}$ (**TTTE**) (**3**) as yellow crystals. Yield: 72%; FT-IR (KBr, cm^{-1}): ν 1680 (C=O), 1615 (C=N), 1575 (C=C); ^1H -NMR ($\text{DMSO-}d_6$): δ 2.36 (s, 6 H, 2 CH_3), 2.44 (s, 6 H, 2 CH_3), 3.25 (s, 6 H, 2 CH_3), 7.19–8.20 (m, 18 H, ArH) ppm; ^{13}C -NMR (100 MHz, $\text{DMSO-}d_6$): δ 11.26 (2 CH_3), 13.84 (2 CH_3), 15.67 (2 CH_3), 121.68, 126.35, 128.92, 129.27, 132.66, 133.70, 138.66, 138.57, 141.17, 142.14, 142.49 (Ar-Cs), 158.00 (C=N), 163.82 (C=O); MS m/z (%): 896 (M^+).

Biological evaluation

Acute toxicity study

Before we examined the biological activity of the **TTTE** compound, an acute toxicity study was carried out to determine the drug's safety. Herein, nine groups were used, each one which was administered with a specific concentration of **TTTE**. *Swiss albino* male mice (6–8 weeks old, 22–26 g weight) were used for an acute toxicity study. After one week of acclimatization, two-fold serial dilution was performed on the **TTTE** starting from 2560 mg/kg body weight (B.W) to 10 mg/kg B.W intraperitoneally (i.p) to give nine groups, and each group contained three mice. Each group was administered the **TTTE** three times for one week, then the mice were monitored for any behavioral signs or mortality for another two weeks. Mice were sacrificed, and liver function tests, aspartate aminotransferase (AST), and alanine transaminase (ALT) (Sclavo Diagnostics International, Italy) were determined^{20,21}.

Liver necrosis using thioacetamide (TAA)

Swiss albino mice with 6–8 weeks old and 22–25 g B.W were used. Mice (from the Animal House of TBRI) were randomly divided into three experimental groups and then the animals were housed for one week. Group-I; the normal control group ($n = 8$), mice received 0.9% w/v of saline i.p. Group-II; TAA control group ($n = 10$), TAA (Sigma Aldrich, Cat. No. 163678) at a dose of 200 mg/kg body weight (B.W) i.p twice per week for eight consecutive weeks to induce liver necrosis. Group-III; **TTTE** treatment group ($n = 30$), as in Group-II the mice were firstly administered with TAA i.p then they were further subdivided into three subgroups to receive treatment with **TTTE** for eight consecutive weeks: Group-IIIa (TAA + **TTTE** 300 mg/kg BW): Mice were treated with **TTTE** at a dose of 300 mg/kg BW three times per week i.p. Group-IIIb (TAA + **TTTE** 200 mg/kg BW): Mice were treated with **TTTE** at a dose of 200 mg/kg BW, three times per week i.p. Group-IIIc (TAA + **TTTE** 100 mg/kg BW): Mice were treated with **TTTE** at a dose of 100 mg/kg BW, three times per week i.p. light anesthesia using a ketamine-xylazine mixture (ketamine 80–100 mg/kg and xylazine 10–12.5 mg/kg), ensuring anesthesia lasts 20–30 min. After the experiment, animals will undergo an 8-hour fasting period before being weighed. Blood samples will be collected from the retro-orbital venous plexus under light anesthesia using a ketamine-xylazine mixture (ketamine 80–100 mg/kg and xylazine 10–12.5 mg/kg), ensuring anesthesia lasts 20–30 min^{22–25}. Table 1.

Molecular detection of liver injury-related markers

Using particularly designed primers, the relative expressions of tissue inhibitor metalloproteinase-1 (TIMP-1) and Cas-3 were evaluated. Extraction of total RNA from liver tissues was carried out using TRIzol reagent (Sigma Aldrich, USA). The RevertAid First Strand cDNA Synthesis Kit (Thermo Fisher, USA) was then used to synthesize cDNA. The primers specified in Table 2 and the Maxima SYBR Green/ROX qPCR Master Mix (2X) (Thermo Fisher, USA) were used for the quantitative PCR (qPCR) studies. The cycling conditions were

Group	Treatment	Dose & Route	Frequency	Duration	n
Group-I	Normal Control	0.9% saline (i.p.)	-	8 weeks	8
Group-II	TAA Control	TAA 200 mg/kg (i.p.)	2×/week	8 weeks	10
Group-IIIa	TAA + TTTE (High Dose)	TTTE 300 mg/kg (i.p.)	3×/week	8 weeks	10
Group-IIIb	TAA + TTTE (Mid Dose)	TTTE 200 mg/kg (i.p.)	3×/week	8 weeks	10
Group-IIIc	TAA + TTTE (Low Dose)	TTTE 100 mg/kg (i.p.)	3×/week	8 weeks	10

Table 1. Experimental design of TAA-induced liver necrosis and TTTE treatment.

Gene	Primer sequence	Accession No.	Reference
B-actin	GCGAATGGGTCAGAAGGACT	>NM_007393.5	[26]
	CTTCTCCATGTCGTCCTCCAGT		
CAS-3	CTACAGGGTTTCATCCAG	NM_007527.4	[27]
	CCAGTTCATCTCCAATTTCG		
TIMP-1	GATATGCCCAACAAGTCCCAGAACC	NM_011593.3	[28]
	GCACACCCACAGCCAGCACTAT		

Table 2. Primer sequence of the determined genes.

as follows: 15 min of initial denaturation at 95 °C, 40 cycles of denaturation at 95 °C for 20 s, and 1 min of annealing/extension at 55 °C. The formula 2^{-ΔΔCt} was used to calculate the relative quantification.

Assessment of Cas-3, TNF-α, NF-κB, and IL-6 levels

Tissue samples were cut into small pieces and then homogenized in 500 μL of phosphate-buffered saline (PBS, pH 7. 4) in the ice using a glass homogenizer. To enhance the disruption of cell membranes, ultrasonication was performed. The homogenates were centrifuged at 1500 g for 15 min to pellet the cell debris from the supernatant. The supernatant was processed for analysis immediately. The level of Cas-3 was measured using a competitive ELISA kit (MyBioSource, USA). Interleukin-6 (IL-6) was quantified using an ELISA kit (RayBiotech, USA). Nuclear Factor kappa B (NF-κB) was detected with an ELISA kit (MyBioSource, USA), while Tumor Necrosis Factor-alpha (TNF-α) was determined using an ELISA kit (Thermo Fisher Scientific, USA).

Histopathological and Immunohistochemical analyses

These analyses were performed in a blinded manner with no knowledge of group type. Samples of isolated livers were promptly fixed in buffered formalin 10%. The liver was exposed to routine paraffin block processing. Under a light microscope, sections were produced and stained with Hematoxylin and Eosin (H&E) to assess hepatic architecture and detect inflammation, dysplasia, and necrosis. A Zeiss Axio microscope was used to compare the liver histology of multiple groups. Images were produced using the attached digital Mrc5 Zeiss camera. An individual sign of liver cell injury was counted in each group in 10 high-power fields (/10 hpf)²⁹.

For immunohistochemical analysis, Sect. 5 μm thick were cut on positively charged glass slides, deparaffinized, hydrated, and then treated for antigen retrieval at a high pH (pH 8) using an automated immunostainer (Dako, Denmark). Monoclonal TGF-β antibody (Cat. No. NHP-AB250, Creative Biolabs, USA) was used as primary antibodies at dilution 1:100. Mouse IgG Fc binding protein conjugated to Horseradish Peroxidase (m-IgG Fc BP-HRP, sc-525409, Abcam UK) was utilized as the secondary antibody at dilution 1:300. Streptavidin–biotin–peroxidase complex and peroxidase-DAB (3,3’diaminobenzidine) (Santa Cruz Biotechnology, USA) detection method was performed according to the manufacturer’s instructions. In each run, positive and negative control slides were included, and a tissue section was processed as described but the primary antibody was omitted³⁰.

Statistical analysis

The study’s data were shown as the mean ± SD. GraphPad Prism 8 (San Diego, CA, USA) was used for performing One-way, two-way ANOVA, or T-test. A p-value of less than 0.05 was considered statistically significant.

Results

Synthesis of 1-(5-((1-(1-(4-((4-(4-(1-((5-acetyl-3-phenyl-1,3,4-thiadiazol-2(3 H)-ylidene)hydrazono)ethyl)-5-methyl-1 H-1,2,3-triazol-1-yl)phenyl)sulfonyl)phenyl)-5-methyl-1 H-1,2,3-triazol-4-yl)ethylidene)hydrazono)-4-phenyl-4,5-dihydro-1,3,4-thiadiazol-2-yl)ethan-1-one (TTTE) (3)
2-(1-(5-methyl-1-(4-((4-(5-methyl-4-(1-(2-((methylthio)carbonothioyl)hydrazono)ethyl)-1H-1,2,3-triazol-1-yl)phenyl)sulfonyl)phenyl)-4,5-dihydro-1H-1,2,3-triazol-4-yl)ethylidene)hydrazine-1-carbodithioate (CPSC) (1) was submitted to react with N-(phenyl)-2-oxopropanehydrazonoyl chloride (2) in ethanol containing catalytic amount of DIPEA to afford the corresponding target molecules 1-(5-((1-(1-(4-((4-(1-((5-acetyl-

3-phenyl-1,3,4-thiadiazol-2(3*H*)-ylidene)hydrazono)ethyl)–5-methyl-1*H*-1,2,3-triazol-1-yl)phenyl)sulfonyl)phenyl)–5-methyl-1*H*-1,2,3-triazol-4-yl)ethylidene)hydrazono)–4-phenyl-4,5-dihydro-1,3,4-thiadiazol-2-yl)ethan-1-one (TTTE) (**3**) in a good yield (Scheme 1). The structure of TTTE was confirmed by spectral data, its ^1H NMR spectrum revealed three singlet signals at δ 2.36, 2.44, and 3.25 ppm attributed to the protons of the sex methyl groups. Additionally, the 18 aromatic protons appeared as multiplet signals in the range from δ 7.19 to δ 8.20 ppm (Fig. 2a). Moreover, its ^{13}C NMR exhibited significant signals at 11.26, 13.84 and 15.67 ppm represented the sex methyl groups carbons and characteristic signals at 121.68, 126.35, 128.92, 129.27, 132.66, 133.70, 138.66, 138.57, 141.17, 142.14, 142.49 for the aromatic carbons, 158.00 for C = N and 163.82 for the C = O (Fig. 2b).

Acute toxicity study

Regarding the acute toxicity study of TTTE, the body weights of the mice in different groups were recorded on day zero and day twenty-one. The highest dose of 2560 mg/kg B. W. was given to the group which had an initial weight of 24.13 ± 2.27 gm on Day 0, which slightly increased to 24.97 ± 1.95 by Day 21. In addition, the group that was administered with the lowest dose of 20 mg/kg B. W. had the least variation with a weight of 18.93 ± 1.3 on Day 0 and 19.7 ± 1.54 gm on Day 21. In general, the groups experienced slight changes in body weight over the 21 days, and no significant weight loss at any of the doses was recorded. No behavioral changes of toxicity were noticed in any of the groups receiving different concentrations of TTTE. The mice were active, did not appear stressed, groomed, and fed normally. Further, there were no changes in the body posture or movement pattern. The absence of any behavioral abnormalities in all experimental groups suggested that TTTE administration did not induce any obvious neurobehavioral toxicity. Fig. 3.

Another confirmation of TTTE safety was liver function tests which revealed that after three weeks of the acute toxicity study, the liver enzyme values were in the normal range in all experimental groups. Table 3.

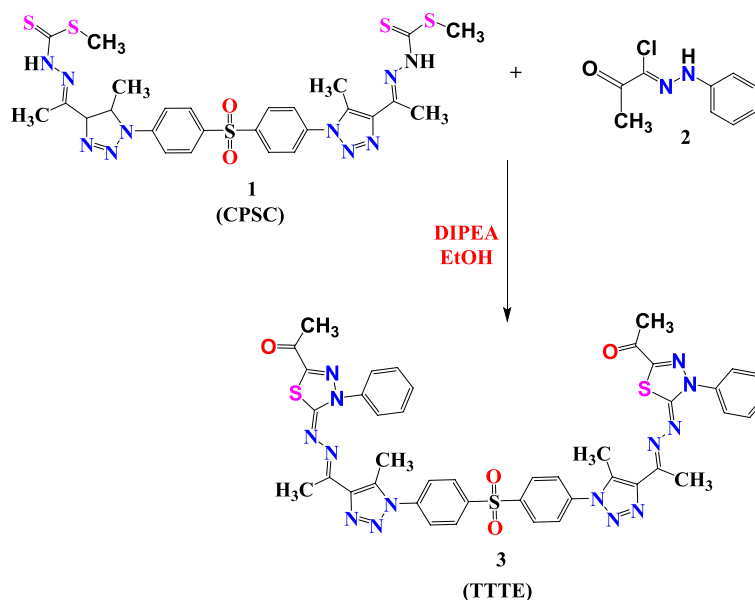
Liver necrosis using thioacetamide (TAA)

Physical parameters

During the experimental study, the death was monitored between groups. Results showed that no mortality was observed in the normal control group (Group-I) with a 100% survival rate. The survival rate for Group-II started to drop at week 4 with a survival rate equal to 40%. Group-IIIa which was treated with a high concentration of TTTE had a survival rate of 62.5%. However, Group-IIIb and Group-IIIc had survival rates of 40% and 30%, respectively. Fig. 4.

Molecular detection of liver injury-related markers

Group-I (normal control) showed a very low expression of Cas-3 and TIMP-1, as expected for a healthy, untreated liver. Group-II (liver necrosis) exhibited a remarked increase in the expression level of Cas-3 with a significantly elevated level of TIMP-1 which indicates a response to tissue injury and attempts at repair or fibrosis in the necrotic liver. Group-IIIa (treated with a high dose of TTTE) showed a substantial reduction in the expression of both TIMP-1 and Cas-3 compared to Group-II. This suggested that the high dose of TTTE possibly had limited tissue damage in the liver, indicating strong therapeutic properties. Group-IIIb (treated with a moderate dose



Scheme 1. Synthetic procedures of 1-(5-((1-(1-(4-((4-(1-((5-acetyl-3-phenyl-1,3,4-thiadiazol-2(3*H*)-ylidene)hydrazono)ethyl)–5-methyl-1*H*-1,2,3-triazol-1-yl)phenyl)sulfonyl)phenyl)–5-methyl-1*H*-1,2,3-triazol-4-yl)ethylidene)hydrazono)–4-phenyl-4,5-dihydro-1,3,4-thiadiazol-2-yl)ethan-1-one (TTTE) (**3**)

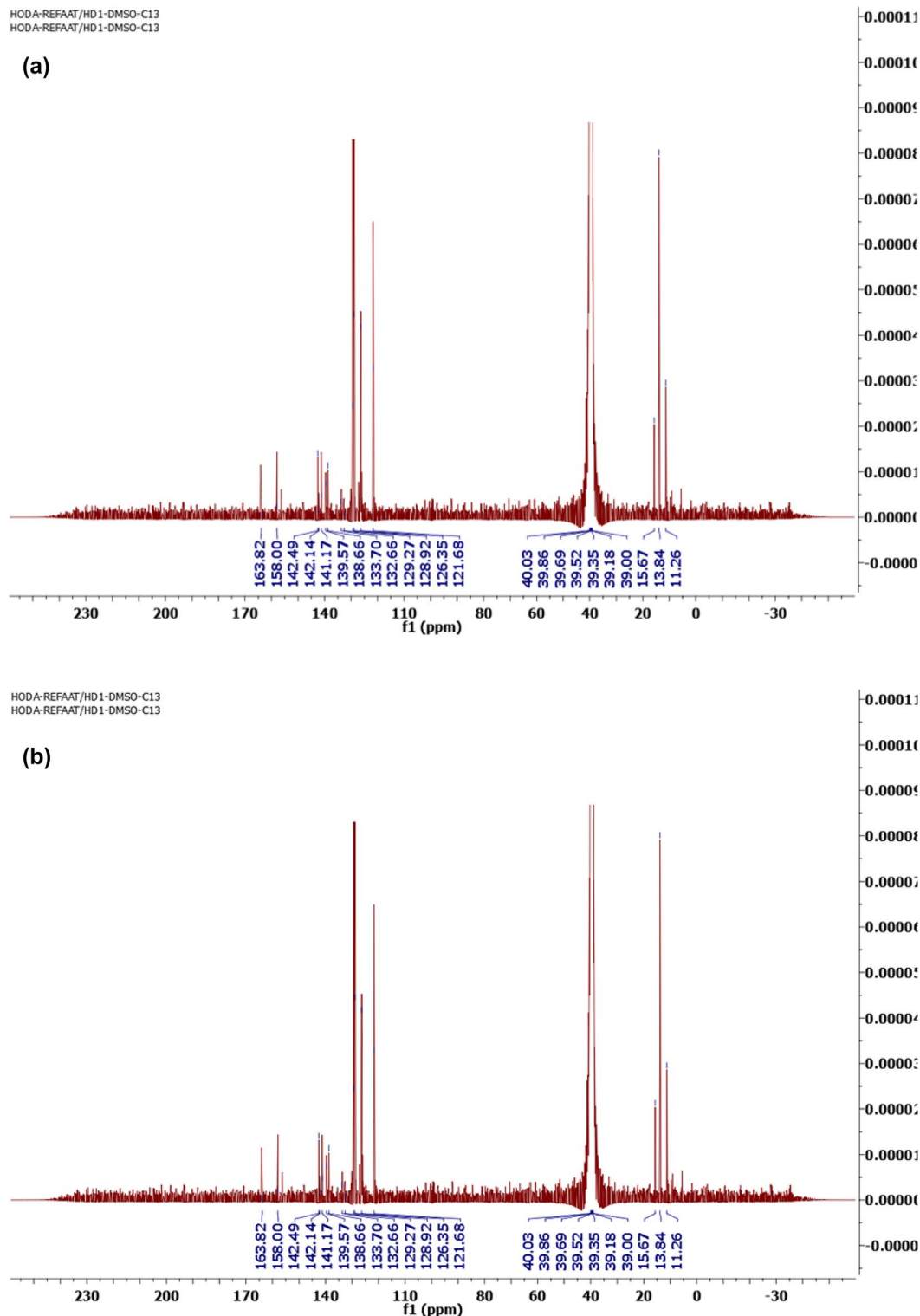


Fig. 2. A ^1H NMR spectrum of 1-(5-((1-(1-(4-((4-(1-((5-acetyl-3-phenyl-1,3,4-thiadiazol-2(3*H*)-ylidene)hydrazono)ethyl)-5-methyl-1*H*-1,2,3-triazol-1-yl)phenyl)sulfonyl)phenyl)-5-methyl-1*H*-1,2,3-triazol-4-yl)ethylidene)hydrazono)-4-phenyl-4,5-dihydro-1,3,4-thiadiazol-2-yl)ethan-1-one (TTTE) (3). B ^{13}C NMR spectrum of 1-(5-((1-(1-(4-((4-(1-((5-acetyl-3-phenyl-1,3,4-thiadiazol-2(3*H*)-ylidene)hydrazono)ethyl)-5-methyl-1*H*-1,2,3-triazol-1-yl)phenyl)sulfonyl)phenyl)-5-methyl-1*H*-1,2,3-triazol-4-yl)ethylidene)hydrazono)-4-phenyl-4,5-dihydro-1,3,4-thiadiazol-2-yl)ethan-1-one (TTTE) (3).

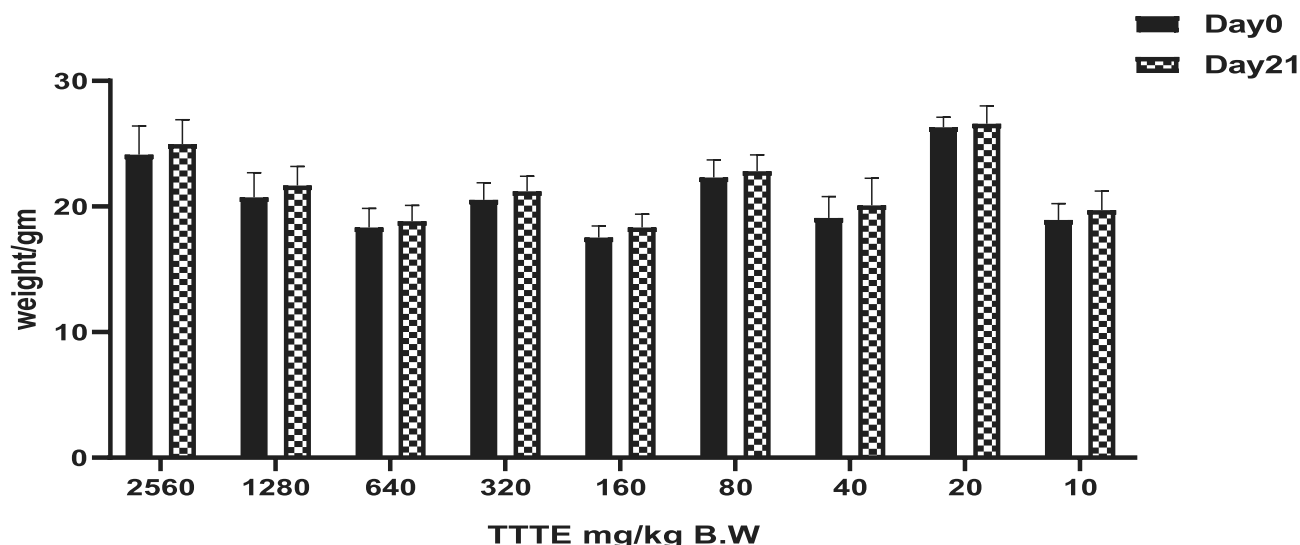


Fig. 3. Body weight monitoring of mice in different TTTE dosage groups over three weeks of acute toxicity study.

IU/L	1	2	3	4	5	6	7	8	9
ALT	42.86±10.04	30.89±12.44	20.68±29.79	27.14±7.99	31.30±9.86	22.34±6.85	25.57±8.68	30.47±14.91	42.66±9.29
AST	79.85±21.96	63.56±10.91	68.44±16.07	72.41±24.94	70.49±21.00	58.95±27.63	57.79±15.95	62.79±12.72	84.85±13.87

Table 3. Liver function tests (ALT/AST) on different acute toxicity groups.

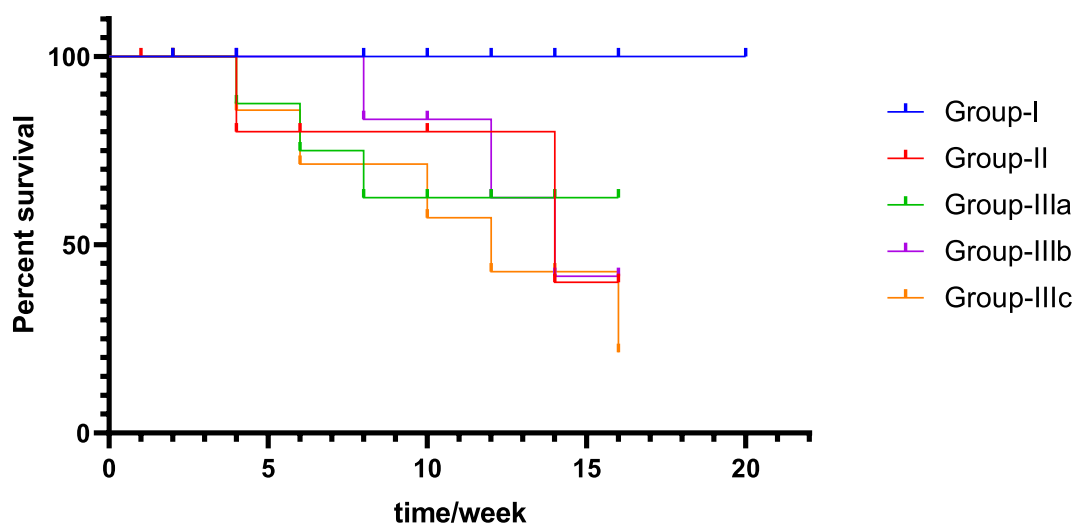


Fig. 4. The graph illustrated here is Kaplan-Meier's survival plot, which explains the probability of survival with time measured in weeks and various groups. On the X-axis, time is measured in weeks; on the Y-axis, the percentage of the survivors is given.

of TTTE) and Group-IIIc (treated with a low dose of TTTE) also showed observed upregulation of Cas-3 and TIMP-1 compared to Group-IIIa. Fig. 5.

Assessment of Cas-3, TNF- α , NF- κ B, and IL-6 Levels

Our findings indicated the change in biochemical parameters related to liver necrosis and the TTTE impact with different concentrations (Fig. 6). Group-II, which is the liver necrosis group, has a significantly higher Cas-3 activity, IL-6, TNF- α as well as the NF- κ B levels compared to the normal group (Group-I) suggesting that apoptosis, inflammation, and activation of the NF- κ B pathway. After TTTE treatment, all three groups IIIa, IIIb,

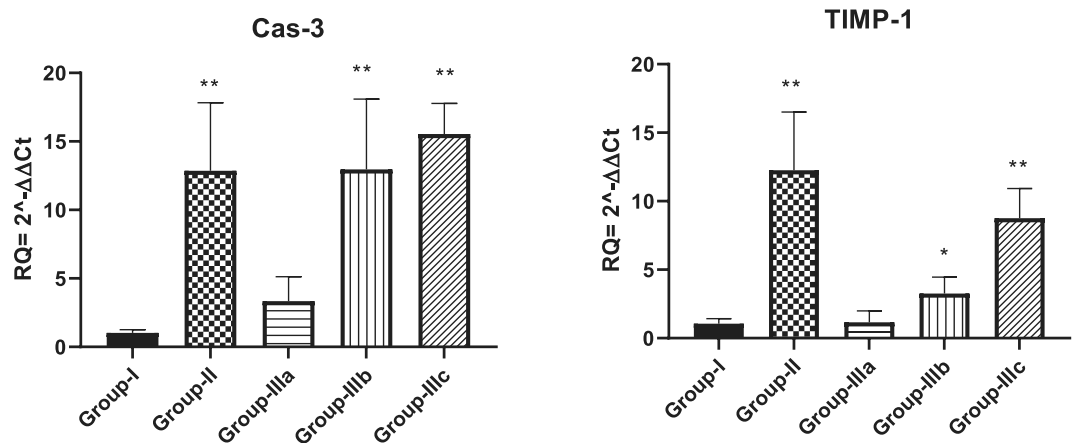


Fig. 5. This bar graph represents the relative expression levels of Cas-3 and TIMP-1 genes. The groups represent different conditions: Group-I (normal control), Group-II (liver necrosis), Group-IIIa (necrosis treated with a high dose of TTTE), Group-IIIb (necrosis treated with a moderate dose of TTTE), and Group-IIIc (necrosis treated with a low dose of TTTE). Data are expressed as mean \pm SEM, with * $p < 0.05$, ** $p < 0.01$, *** $p < 0.001$, and **** $p < 0.0001$ compared to Group-I.

and IIIc showed a decrease in these markers in a dose-dependent manner. High-dose TTTE treatment (Group-IIIa) significantly affects caspase-3 activity, IL-6, TNF- α , and NF- κ B levels near the normal group showing the protective and anti-inflammatory effect. Group-IIIb and IIIc also exhibited a decrease in these markers, though lesser than Group-IIIa showing that TTTE had a therapeutic effect on liver necrosis although not as potent as the high dose.

Histopathological Examination

In the TAA-treated group, liver injury was characterized by spotty necrosis and mild to moderate interface hepatitis with a few foci of bridging portal–portal inflammation. However, no confluent necrosis, bridging inflammation, or fibrosis was observed in this group. Group-IIIa, treated with 300 mg of TTTE, exhibited no signs of hepatocyte injury or fibrosis. Group-IIIb, treated with 200 mg of TTTE, showed multiple spotty necrosis, focal confluent necrosis, and moderate to severe interface hepatitis. Additionally, there were few foci of bridging inflammation (portal–portal, and portal–central) and minimal periportal fibrosis, as well as fibrosis surrounding necrotic nodules. In Group-IIIc, treated with the lowest TTTE dose (100 mg), multiple spotty necrosis was observed without confluent necrosis. However, mild to moderate interface hepatitis, frequent foci of bridging inflammation (portal–portal, and portal–central), and frequent foci of bridging fibrosis were present, though no frank cirrhotic nodules were detected. (Fig. 7a and b)

Spotty necrosis score (/10 hpf) showed that both TAA and the lowest TTTE dose groups had the highest spotty necrosis scores; 6.17 ± 2 and 7.17 ± 3.3 , respectively. Group-IIIa treated with 300 mg of TTTE had the lowest spotty necrosis score (0.67 ± 0.5) with statistical significance correlated to Group-II, p -value = 0.0045.

Immunohistochemical analysis

Results of immunohistochemistry showed that both the moderated and low-dose TTTE-treated group (Group-IIIb and Group-IIIc) in addition to the TAA group had an obvious.

TGF- β expression which indicates an active inflammatory response. However, no expression of TGF- β was observed in the high-dose TTTE-treated group (Group-IIIa). These data are compatible with H & E in addition to Massone trichrome stains. Fig. 8.

Discussion

In this study, we evaluated the potential therapeutic efficacy of TTTE in the treatment of liver necrosis induced by thioacetamide (TAA) in mice model. Our findings showed that B.W., in addition to the survival rate in the TAA group, remarkably decreased (40%). A 62.5% was shown in the high-dose TTTE-treated group, indicating the potential therapeutic efficacy of TTTE at this concentration (300 mg/Kg B.W). The moderate-dose (40%) and low-dose (30%) were considerably lower, which proved that lower concentrations of TTTE lack the potency to increase the survival percentage or to reduce the damaging effects observed in the TAA group. Like other chalcone hepatoprotectants, our derivative required higher concentrations (40%) to significantly improve survival, while lower doses (30%) showed negligible effects. Unlike classical chalcones³¹, the bis-sulfone moiety in TTTE may alter its dose-response profile, explaining the observed threshold effect^{32,33}. Caspase-3 (Cas-3) is one of the most important enzymes involved in liver necrosis, especially in cases of apoptosis-mediated cell death. In liver necrosis, the activation of caspase-3 is essential in the apoptotic signaling cascade since it affects the liver's capacity to regenerate^{34,35}. Herein, the TTTE compound reduced the expression of genes associated with apoptosis; Cas-3, and TIMP-1 in a dose-dependent manner, showing that higher doses had an impact on liver injury treatment by reducing cell death and fibrogenesis. While the present study focused on transcriptional

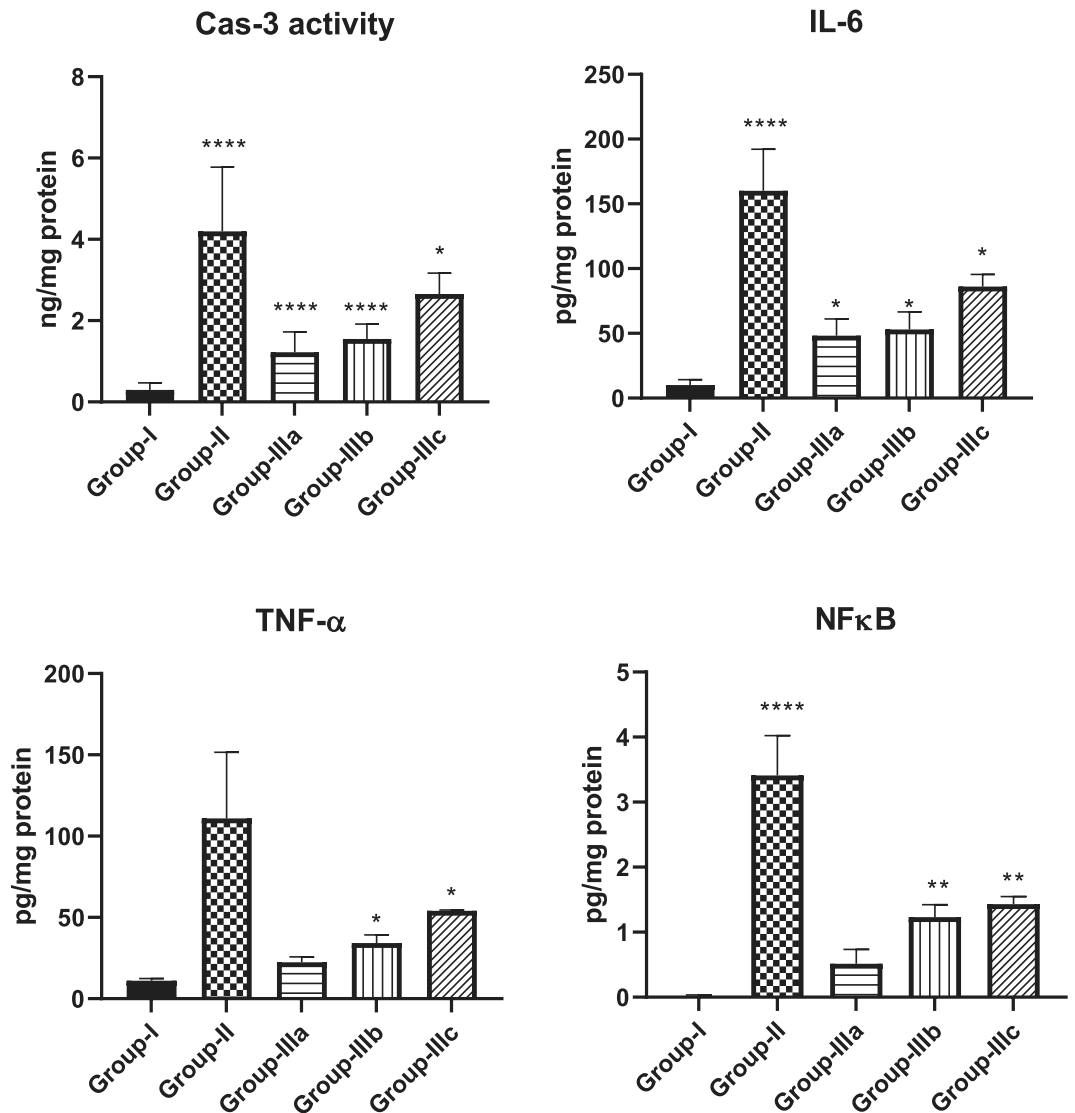


Fig. 6. Effect of TTTE treatment on biochemical markers in liver necrosis (Caspase-3 activity, IL-6, TNF- α , and NF- κ B levels). Data are expressed as mean \pm SEM, with * p < 0.05, ** p < 0.01, *** p < 0.001, and **** p < 0.0001 compared to Group-I.

profiling of TIMP-1, we acknowledge that mRNA expression may not always reflect actual protein levels due to post-transcriptional regulation. Nevertheless, the observed mRNA expression patterns are consistent with established responses in liver injury models, where TIMP-1 upregulation is associated with fibrogenesis and tissue remodeling. The significant downregulation of TIMP-1 mRNA in TTTE-treated groups, particularly at the high dose, indicates a probable attenuation of fibrotic activity^{36,37}. The results displayed a dosage-dependent decrease in essential inflammatory mediators TNF- α and NF- κ B after TTTE treatment. TNF- α serves as a known apoptosis trigger of hepatocytes³⁸, in addition, the activation of NF- κ B sustains inflammatory cascades in liver injury, thus, their suppression potentially leads to decreased liver necrosis³⁹. Our results showed a significant reduction in the levels of TGF- β , which stands as a central cytokine during fibrogenesis processes. TGF- β drives the development of liver fibrosis when it activates hepatic stellate cells (HSCs) that produce and deposit excessive ECM and collagen⁴⁰. The downregulation of these critical profibrotic and pro-inflammatory markers suggests that TTTE exerts its hepatoprotective effects through multimodal mechanisms, targeting both necroinflammation and fibrotic progression. In our study, immunohistochemistry analysis on liver tissue treated with a low dose of the TTTE revealed the presence of TGF- β expression, indicating fibrosis activation. Also, H & E in addition to Masson trichrome revealed the same results by showing multiple spotty necrosis with moderate interface hepatitis, frequent foci of bridging inflammation (portal–portal, and portal–central), and frequent foci of bridging fibrosis. This suggests that the low dose may not be sufficient to fully inhibit liver injury; in tissues treated with moderate and high doses of the TTTE, no TGF- β expression was observed. These results suggest a mitigation of fibrogenic activity, although this reduction may not be sufficient to fully reverse established fibrosis, but likely contributes to slowing or halting the progression of fibrotic remodeling by attenuating HSC activation

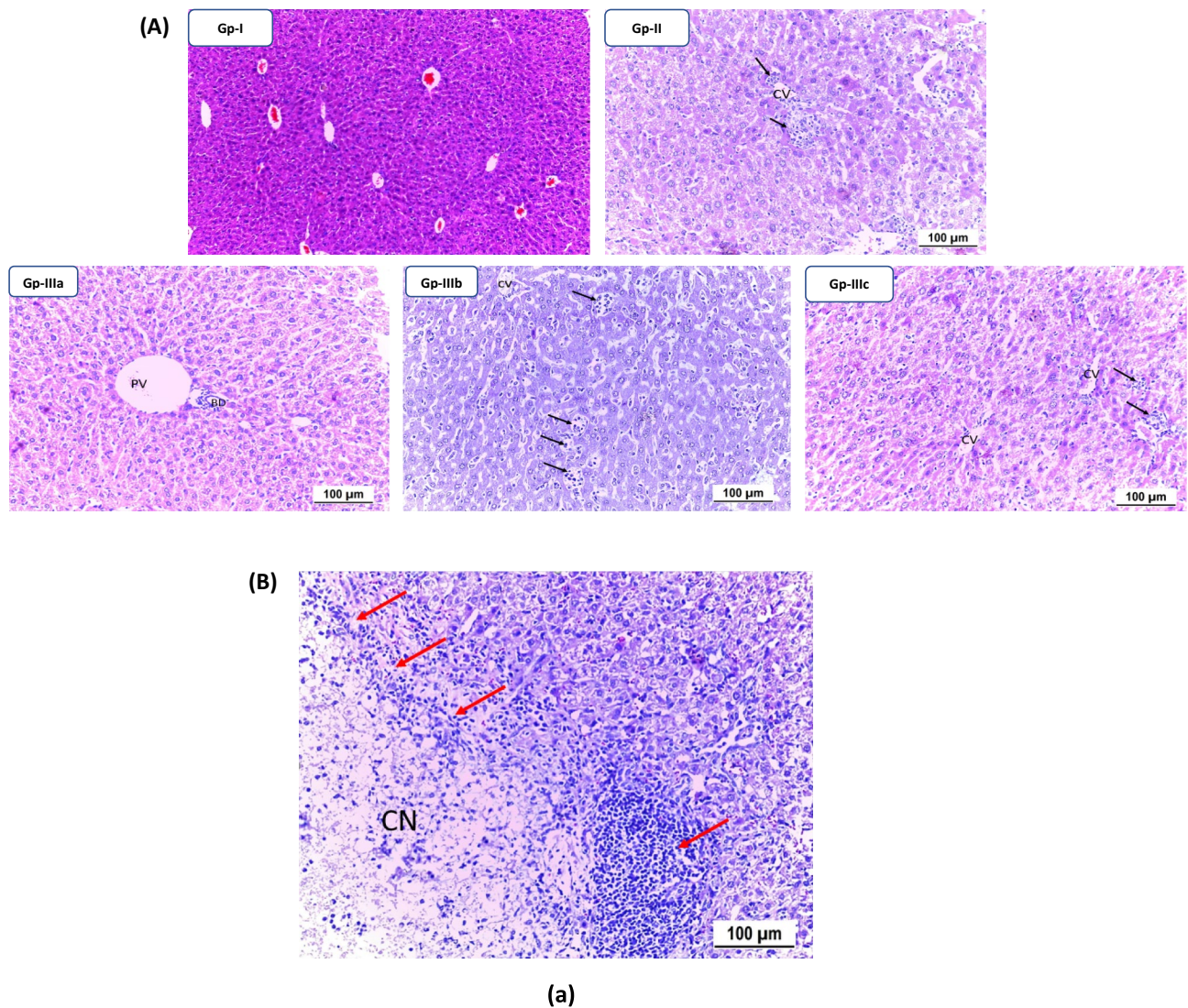


Fig. 7. **A** Spotty necrosis detection (H & E stain) of mice liver tissue of different groups at low magnification power; spotty necrosis (black arrows); CV: central vein, PV: portal vein, BD: bile duct. Both normal and treated with high-dose TTTE groups (Group-I and Group-IIIa) showed no signs of liver cell injury with normal portal triad in addition to appearing hepatocytes with preserved configuration. TAA group (Group-II), moderate-dose and low-dose TTTE groups; Group-IIIb & Group-IIIc showed multiple spotty necrosis. **B** H & E stain of mice liver tissue; PV: portal vein, BD: Bile duct, CV: Central vein. (a) Confluent necrosis (CN) and surrounding lymphocytic infiltrate (red arrows) in low-dose TTTE group (Group-IIIc). (b): Mild interface hepatitis (red arrowhead) was observed in TAA group (Group-II) with spotty necrosis (black arrow) and moderate interface hepatitis was observed in moderate-dose TTTE group (Group-IIIb). (c): H & E stain of low-dose TTTE group (Group-IIIc) showed portal-portal bridging hepatitis (double head red arrow) and portal-central bridging hepatitis (double head black arrow). Masson trichrome staining showed evolving portal–portal bridging fibrosis with early nodular formation (dotted) in addition to evolving fibrous tissue deposited in sinusoid around hepatocytes.

and ECM deposition⁴¹. These results recommended that high-dose of TTTE potentially reduce inflammation via downregulation of TNF- α and NF- κ B, which play critical roles in hepatocyte apoptosis and chronic liver inflammation, in alignment with our experimental findings, which could accelerate fibrogenic processes.

Conclusion

A study examined the hepatoprotective effect of TTTE, which is a modern sulfone-bis chalcone derivative, through laboratory tests on thioacetamide (TAA)-induced liver necrosis mouse subjects. The protection offered by TTTE depends on the dosage because it leads to better survival results and lessened tissue damage with a substantial decrease in the markers for cellular death and inflammation, such as Caspase-3, TNF- α , and NF- κ B. The high dosage treatment with TTTE blocked fibrogenic signals since no TGF- β was detected in liver tissue alongside decreased fibrosis. These findings highlight the therapeutic relevance of chalcone-based compounds,

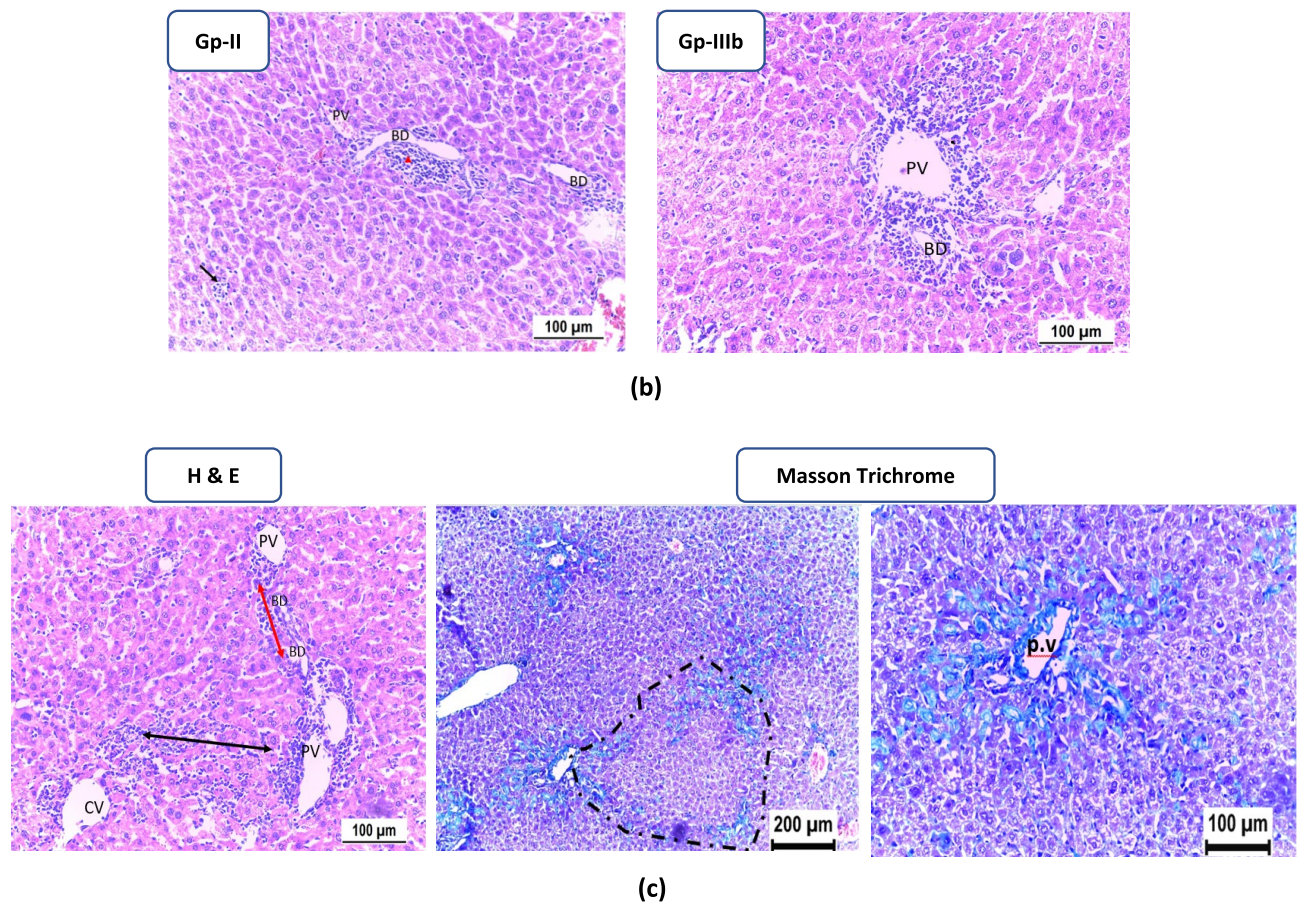


Fig. 7. (continued)

particularly sulfone-bis chalcone derivatives like TTTE, in managing liver injury and fibrosis. The anti-apoptotic, anti-inflammatory, and anti-fibrotic properties observed in this study support TTTE's potential as a promising candidate for further preclinical development. As interest in chalcone scaffolds continues to grow due to their diverse biological activities, this compound adds valuable insight into their possible application in liver disease therapy.

Limitations and future perspectives

The study has various limitations, even with its promising results. We noticed that higher doses correlated with reduced TIMP-1 and Caspase-3 mRNA expression but we failed to obtain protein data at the same time. Fundamental research utilizing Western blotting and related analytical methods like ELISA and immunofluorescence must be done to verify these transcriptional modifications at the protein expression level. The relevance of using TAA-induced liver injury models in mice remains unclear when aiming to understand hepatotoxicity and fibrosis patterns in human patients because additional research into chronic liver models and clinical sample analysis is mandatory. The observations of survival rates in addition to the sample sizes need larger numbers of test subjects particularly within the low- and moderate-dose groups to establish statistical validity. Functional assessments measuring liver health such as ALT, AST liver enzyme levels, and bilirubin content in blood and oxidative stress markers should be added to future evaluations of TTTE due to their omission from the current investigation. Future studies on TTTE are required to determine its pharmacokinetic data, long-term safety, and molecular mechanism of action in detail. Expanding the assessment of TTTE's therapeutic value includes tests for its performance in models of NASH and viral hepatitis conditions. Further research should explore whether combining TTTE with present-day hepatoprotective agents would generate combined therapeutic results that would promote innovative treatment method development. Translation studies, along with clinical trials, represent the essential basis for developing TTTE into a new therapeutic agent that might treat chronic liver diseases in people.

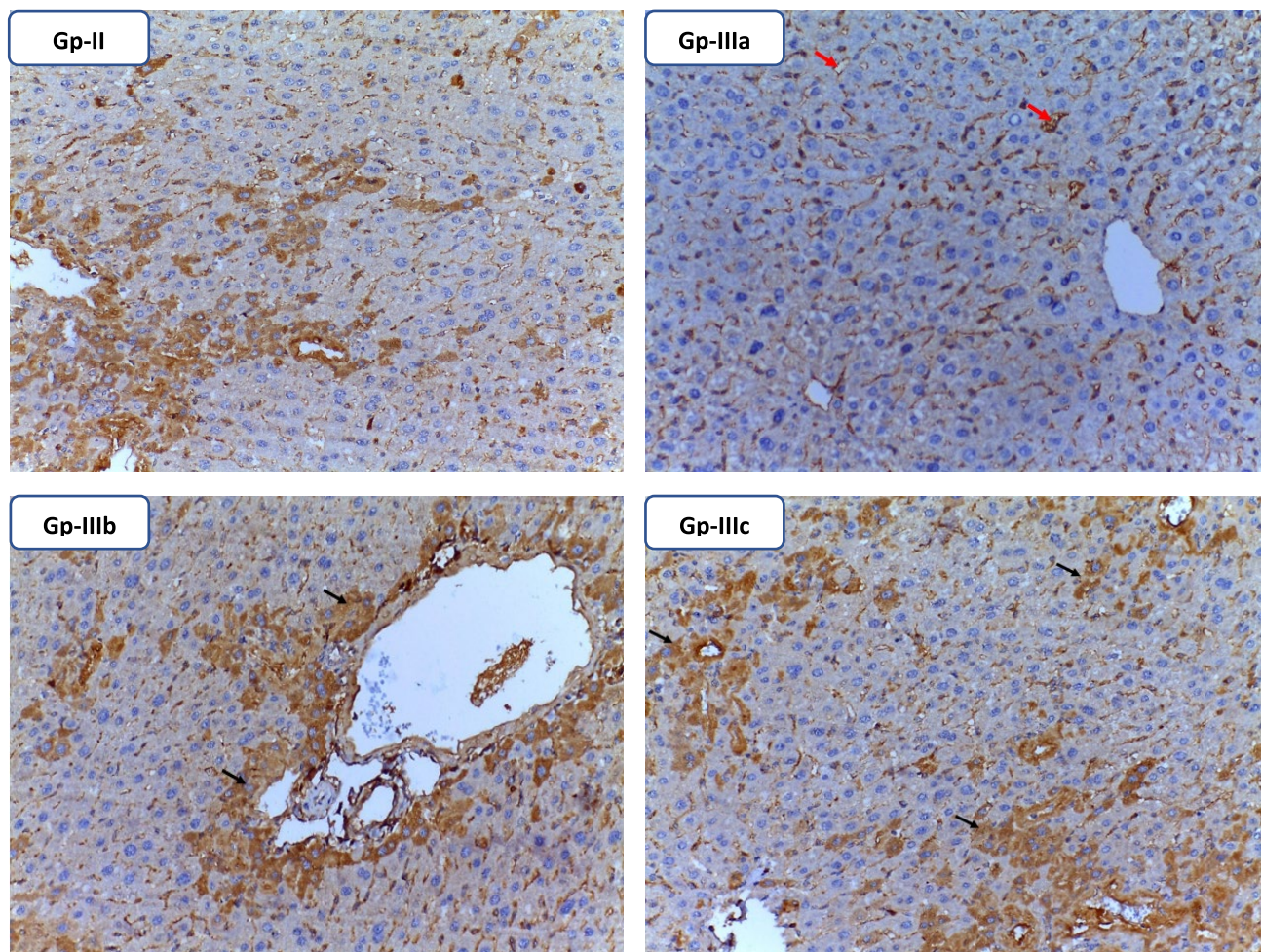


Fig. 8. Immunohistochemical analysis of TGF- β expression in liver tissue stained with TGF- β antibody. In the TAA group (Gp-II), Gp-IIIb, and Gp-IIIc showed scattered cytoplasmic positivity in hepatocytes (black arrows). The high TTTE-treated group; Gp-IIIa, showed hepatocytes with a negative TGF- β immunohistochemical stain. Red arrows revealed non-specific immunohistochemical staining in the liver sinusoidal. (x20).

Data Availability

all the data used are included in the manuscript

Received: 30 January 2025; Accepted: 13 May 2025

Published online: 20 May 2025

References

- Asrani, S. K., Devarbhavi, H., Eaton, J. & Kamath, P. S. Burden of liver diseases in the world. *J. Hepatol.* **70**, <https://doi.org/10.1016/j.jhep.2018.09.014> (2019).
- World Health Organization. *Global Hepatitis Report 2017* (World Health Organization, 2017).
- Huang, D. Q., El-Serag, H. B. & Loomba, R. Global epidemiology of NAFLD-related HCC: trends, predictions, risk factors and prevention. *Nat. Rev. Gastroenterol. Hepatol.* **18**, <https://doi.org/10.1038/s41575-020-00381-6> (2021).
- Nojoomi, F., Ghasemian, A., Fallahi, S. & Hasanvand, F. High prevalence and risk factors of hepatitis B, C and E infections among Middle Eastern countries. *Immunopathol. Persa* **4**, <https://doi.org/10.15171/ipp.2018.18> (2018).
- Ramalingappa, P., Aradhya, H., Hanumantharaya, N. & Bolarigowda, P. Alpha Methyl dopa induced hepatotoxicity in pregnancy. *Int. J. Reprod. Contracept. Obstet. Gynecol.* **3**, 805–807. <https://doi.org/10.5455/2320-1770.ijrcog20140938> (2014).
- Böttcher, K. & Pinzani, M. Pathophysiology of liver fibrosis and the methodological barriers to the development of anti-fibrogenic agents. *Adv. Drug Deliv. Rev.* **121**, 3–8. <https://doi.org/10.1016/j.addr.2017.05.016> (2017).
- Chatila, R. Hepatotoxicity: The Adverse Effects of Drugs and Other Chemicals on the Liver. *J. Clin. Gastroenterol.* **31**, <https://doi.org/10.1097/00004836-200009000-00024> (2000).
- Weng, H. et al. Two sides of one coin: massive hepatic necrosis and progenitor cell-mediated regeneration in acute liver failure. *Front. Physiol.* **6**, <https://doi.org/10.3389/fphys.2015.00178> (2015).
- Rennebaum, F. & Trebicka, J. Acute liver failure. *Tagliche Prax.* **67**, 590–600. https://doi.org/10.30856/th.jhep2018vol1iss1_63 (2023).
- Forrest, J. A. H., Clements, J. A. & Prescott, L. F. Clinical pharmacokinetics of Paracetamol. *Clin. Pharmacokinet.* **7**, 93–107. <https://doi.org/10.2165/00003088-198207020-00001> (1982).

11. Aryasa, I. W. T. & Noviandri, I. Voltammetric determination of Paracetamol with carbon paste electrode modified with molecularly imprinted electropolymer. *Molekul* **17**, 30–38. <https://doi.org/10.20884/1.jm.2022.17.1.5595> (2022).
12. Laine, J. E., Auriola, S., Pasanen, M. & Juvonen, R. O. Acetaminophen bioactivation by human cytochrome P450 enzymes and animal microsomes. *Xenobiotica* **39**, 11–21. <https://doi.org/10.1080/00498250802512830> (2009).
13. Yan, Y., Zeng, J., Xing, L. & Li, C. Extra- and Intra-Cellular mechanisms of hepatic stellate cell activation. *Biomedicine* **9**, 1014. <https://doi.org/10.3390/biomedicine9081014> (2021).
14. Garbuzenko, D. V. Pathophysiological mechanisms of hepatic stellate cells activation in liver fibrosis. *World J. Clin. Cases* **10**, 3662. <https://doi.org/10.12998/WJCC.V10.I12.3662> (2022).
15. Abdelrahman, H., Ajaj, A., Atique, S., El-Menyar, A. & Al-Thani, H. Conservative management of major liver necrosis after angioembolization in a patient with blunt trauma. *Case Rep. Surg.* **2013**, 1–4. <https://doi.org/10.1155/2013/954050> (2013).
16. Zou, L. et al. Downregulation of SLC7A11 by Bis(4-Hydroxy-3,5-Dimethylphenyl) sulfone induces ferroptosis in hepatocellular carcinoma cell. *Mol. Carcinog.* **64**, 580–596. <https://doi.org/10.1002/mc.23874> (2025).
17. Matic, J. et al. Sulfone-based human liver pyruvate kinase inhibitors - Design, synthesis and in vitro bioactivity. *Eur. J. Med. Chem.* **269**, 116306. <https://doi.org/10.1016/j.ejmech.2024.116306> (2024).
18. Radwan, E. K. et al. Synthesis and application of a new multi-functional biopolymer-based aerogel loaded with bistriazole derivative as highly efficient adsorbent and disinfectant. *J. Clean. Prod.* **434**. <https://doi.org/10.1016/j.jclepro.2023.139932> (2024).
19. hanaa, F. et al. Design, efficient synthesis, mechanism of reaction and antiproliferative activity against cancer and normal cell lines of a novel class of fused pyrimidine derivatives, *Acta Pol. Pharm. Res.* **75** (2018).
20. Rameshwar, G. S., Venkatrao, P. U., Vithalrao, N. A. & Pramodrao, A. M. OECD GUIDELINES FOR ACUTE ORAL TOXICITY STUDIES: AN OVERVIEW. *Int. J. Res. Ayurveda Pharm.* **14**, 137–140. <https://doi.org/10.7897/2277-4343.1404130> (2023).
21. Tran, P. N. T. & Tran, T. T. N. Evaluation of acute and subchronic toxicity induced by the crude ethanol extract of *Plukenetia volubilis* Linneo leaves in Swiss albino mice. *Biomed. Res. Int.* **2021**, 6524658. <https://doi.org/10.1155/2021/6524658> (2021).
22. Fahmi, M. Z. et al. In vivo study of chalcone loaded carbon Dots for enhancement of anticancer and bioimaging potencies. *Nanotheranostics* **7**, 281–298. <https://doi.org/10.7150/ntno.80030> (2023).
23. Wallace, M. et al. Standard Operating Procedures in Experimental Liver Research: Thioacetamide model in mice and rats. *Lab. Anim.* **49**. <https://doi.org/10.1177/0023677215573040> (2015).
24. Salehi, B. et al. Pharmacological Properties of Chalcones: A Review of Preclinical Including Molecular Mechanisms and Clinical Evidence. *Front. Pharmacol.* **11**. <https://doi.org/10.3389/fphar.2020.592654> (2021).
25. Abdelmonsef, A. H. et al. A search for antiinflammatory therapies: synthesis, in Silico investigation of the mode of action, and in vitro analyses of new quinazolin-2, 4-dione derivatives targeting phosphodiesterase-4 enzyme. *J. Heterocycl. Chem.* **59**, 474–492 (2022).
26. Lei, Y. et al. CHOP favors Endoplasmic reticulum stress-induced apoptosis in hepatocellular carcinoma cells via Inhibition of autophagy. *PLoS One* **12**, 1–17. <https://doi.org/10.1371/journal.pone.0183680> (2017).
27. Ghatei, N. et al. Evaluation of Bax, bcl-2, p21 and p53 genes expression variations on cerebellum of BALB/c mice before and after birth under mobile phone radiation exposure. *Iran. J. Basic. Med. Sci.* **20**, 1037. <https://doi.org/10.22038/IJBMS.2017.9273> (2017).
28. Meissburger, B., Stachorski, L., Röder, E., Rudofsky, G. & Wolfrum, C. Tissue inhibitor of matrix metalloproteinase 1 (TIMP1) controls adipogenesis in obesity in mice and in humans. *Diabetologia* **54**, 1468–1479. <https://doi.org/10.1007/s00125-011-2093-9> (2011).
29. Drury, R. & Techniques Theory and Practice of Histological *J. Clin. Pathol.* **36** 609–609. <https://doi.org/10.1136/jcp.36.5.609-d> (1983).
30. Malatesta, M. Histological and Histochemical Methods - Theory and practice. *Eur. J. Histochem.* **60**. <https://doi.org/10.4081/ejh.2016.2639> (2016).
31. Mahapatra, D. K., Asati, V. & Bharti, S. K. Chalcones and their therapeutic targets for the management of diabetes: Structural and pharmacological perspectives. *Eur. J. Med. Chem.* **92**. <https://doi.org/10.1016/j.ejmech.2015.01.051> (2015).
32. Singh, H., Sidhu, S., Chopra, K. & Khan, M. U. Hepatoprotective effect of trans-Chalcone on experimentally induced hepatic injury in rats: Inhibition of hepatic inflammation and fibrosis. *Can. J. Physiol. Pharmacol.* **94**, 879–887. <https://doi.org/10.1139/cjpp-2016-0071> (2015).
33. Karimi-Sales, E., Mohaddes, G. & Alipour, M. R. Chalcones as putative hepatoprotective agents: preclinical evidence and molecular mechanisms. *Pharmacol. Res.* **129**, 177–187. <https://doi.org/10.1016/j.phrs.2017.11.022> (2018).
34. Thapaliya, S. et al. Caspase 3 inactivation protects against hepatic cell death and ameliorates fibrogenesis in a diet-induced NASH model. *Dig. Dis. Sci.* **59**, 1197–1206. <https://doi.org/10.1007/s10620-014-3167-6> (2014).
35. Shojaie, L., Iorga, A. & Dara, L. Cell death in liver diseases: A review. *Int. J. Mol. Sci.* **21**, 1–47. <https://doi.org/10.3390/ijms21249682> (2020).
36. Iredale, J. P. Models of liver fibrosis: Exploring the dynamic nature of inflammation and repair in a solid organ. *J. Clin. Invest.* **117**. <https://doi.org/10.1172/JCI30542> (2007).
37. Murawaki, Y., Ikuta, Y., Idobe, Y., Kitamura, Y. & Kawasaki, H. Tissue inhibitor of metalloproteinase-1 in the liver of patients with chronic liver disease. *J. Hepatol.* **26**, 1213–1219. [https://doi.org/10.1016/S0168-8278\(97\)80454-0](https://doi.org/10.1016/S0168-8278(97)80454-0) (1997).
38. Van Antwerp, D. J., Martin, S. J., Kafri, T., Green, D. R. & Verma, I. M. Suppression of TNF- α -induced apoptosis by NF- κ B. *Sci.* (80-). **274**, 787–789. <https://doi.org/10.1126/science.274.5288.787> (1996).
39. Sun, B. & Karin, M. NF- κ B signaling, liver disease and hepatoprotective agents. *Oncogene* **27**, 6228–6244. <https://doi.org/10.1038/onc.2008.300> (2008).
40. Aoyama, T., Paik, Y.-H. & Seki, E. Toll-Like receptor signaling and liver fibrosis. *Gastroenterol. Res. Pract.* **2010**, 1–8. <https://doi.org/10.1155/2010/192543> (2010).
41. Lee, U. E. & Friedman, S. L. Mechanisms of hepatic fibrogenesis, *Best Pract. Res. Clin. Gastroenterol.* **25**. <https://doi.org/10.1016/j.bpg.2011.02.005> (2011).

Author contributions

All the authors (HRMR; SH; SM and HO) have write and reviewed the manuscript

Funding

Open access funding provided by The Science, Technology & Innovation Funding Authority (STDF) in cooperation with The Egyptian Knowledge Bank (EKB).

Declarations

Competing interests

The authors declare no competing interests.

Ethical approval

The protocol of this study was approved by Research ethical committee of Theodor Bilharz Research Institute, No: PT (824). All animal studies were performed according to the principles of the Institutional Ethical Committee guidelines for treating experimental animals (FWA 00010609). The study investigated the impacts of the TTTE compound on necrosis in addition to fibrosis. This adjustment enabled an assessment of TTTE's therapeutic efficacy for liver injury treatment.

Additional information

Correspondence and requests for materials should be addressed to H.R.M.R.

Reprints and permissions information is available at www.nature.com/reprints.

Publisher's note Springer Nature remains neutral with regard to jurisdictional claims in published maps and institutional affiliations.

Open Access This article is licensed under a Creative Commons Attribution-NonCommercial-NoDerivatives 4.0 International License, which permits any non-commercial use, sharing, distribution and reproduction in any medium or format, as long as you give appropriate credit to the original author(s) and the source, provide a link to the Creative Commons licence, and indicate if you modified the licensed material. You do not have permission under this licence to share adapted material derived from this article or parts of it. The images or other third party material in this article are included in the article's Creative Commons licence, unless indicated otherwise in a credit line to the material. If material is not included in the article's Creative Commons licence and your intended use is not permitted by statutory regulation or exceeds the permitted use, you will need to obtain permission directly from the copyright holder. To view a copy of this licence, visit <http://creativecommons.org/licenses/by-nc-nd/4.0/>.

© The Author(s) 2025